Preparation of Functionalized Sodium carboxymethyl cellulose/Sodium alginate-Based Tween (80) for Potential Allocation of Linezolid as Antimicrobial Agents

Afaf Adel El-bana (afafelbana551@gmail.com)
Higher Institute of Engineering and Technology at Manzala https://orcid.org/0000-0001-5963-2756
Amr Mohamed Abdelghany
Mahrous Shaker Meikhail

Research Article

Keywords: Sodium carboxymethyl cellulose, Sodium alginate, Linezolid drug, FTIR, XRD, UV/Vis, SEM, Antibacterial activity

Posted Date: April 12th, 2022

DOI: https://doi.org/10.21203/rs.3.rs-1531127/v1

Abstract

Innovative adhesive bio-films were developed for antimicrobial wound bandages. The bio-films are prepared by blending natural polymers such as sodium carboxymethyl cellulose and sodium alginate with a surfactant as Tween(80) and loaded with Linezolid drug as antimicrobial agents. In this paper, polymeric films were prepared by casting film-forming method. Prefatory studies comprised XRD, FTIR, UV/vis spectroscopy, and SEM to specify lattice structure, interactions, optical properties, and morphology. Antibacterial analysis was also performed by agar well diffusion tests. The effect of bio-film composition on *E.coli*, *P.aeuroginosa, S.aureus*, *B.subtilis* standard bacteria, and *C.albicans* pathogenic fungus was studied and compared with biomaterial film without Linezolid drug. The in vitro antibacterial assay of bio-films formulations was assessed in bacterial and fungal strains, showing a significant activity over time rather than control bio-film. Finally, the preparation of biomaterial films loaded with Linezolid drug (antimicrobial wound dressings) is an environmentally friendly solution that may contribute to the development of wound healing.

1. Introduction

Till presently wound dressing is an unmet contest amidst pharmaceutical and operational society. Indeed, chronic and post-traumatic wounds can be deadly in several situations since they manage to be settled effortlessly by renitent microorganisms like bacteria and germs. Diverse bandages were furnished to coat the wound superficies to be an appropriate hurdle against injury contagion [1, 2].

Native antibiotics can perform a significant function to avert and cure various dominant dermal pathogenic contagions such as regional superficial contagions owing to trauma, and abrasion. Linezolid is an antibacterial agent that is forcefully used for the treatment of complicated skin and skin structure infections (SSSIs), including diabetic foot infections (DFIs) without concomitant osteomyelitis averse to wound pathogens inclusive Methicillin-Resistant Staphylococcus aureus (MRSA) [3].

Linezolid was identified chemically as (S)-N-[[3-(3fluoro-4-morpholinylphenyl)-2-oxo-5-oxazolidinyl] methyl] acetamide which meditated as the first member of the class of oxazolidinone antibiotics that performs by inhibiting the initiation of bacterial protein synthesis and terrific pharmacokinetic index [3, 4].

Latterly, antimicrobial systems based on bio-polymeric infrastructure are being inspected to remedy the impedance of antimicrobial troubles and ascertain a valid solution for the strengthening of the interaction between antibiotics and bacterial cell barriers.

It is renowned that naturally occurred sodium carboxymethyl cellulose (Na-CMC); is very hydrophilic (water affinity) due to the presence of numerous hydroxyl (-OH) and carboxyl (-COOH) groups. Na-CMC has exceptional characteristics due to its low price, the ability to form films when fused with semi-crystalline polymers or with crosslinking agent support, super water-solubility, and better biocompatibility, best-swelling capability (in saline solutions and distilled water), equilibrium water uptake, and abundance [5, 6]. However, assigning to its hydrophilicity, less mechanical properties, and low adsorption. These

downsides may be conquered by a suitably blended tweaking to refine utility and implant coating application. The choice polymer for blending is sodium alginate (Na-Alg) due to natural casings, high availability, moisture reservation, gel-forming capability, excellent biocompatibility, higher molecular weight, safe, perishable, non-immunogenic, and higher viscosity [7].

However, the bio-polymeric infrastructure still has drawbacks due to less flexibility of Na-Alg which affected the mechanical properties. Therefore, added surfactants such as Tween(80), To deliver the bio-film to the desired qualities such as flexibility or elasticity (enhance mechanical properties), delay erosion, water adsorption, and gaseous exchange refinement. Tween(80) has a high hydrophilic/lipophilic balance (HLB), which means the hydrophilic fraction with the hydrophilic film matrix may lessen water binding sites quantities while the hydrophobic fraction may perform as a water vapor permeability (WVP) barrier [8, 9]. However; the bio-polymeric infrastructure (Na-CMC/Na-Alg/Tween(80)) still does not include all the specifications of the distinctive bandage for wounds due to antimicrobial activity drawbacks (no activity) against gram-positive, gram-negative, and fungi. So, this dressing will permit bacterial contamination and imbibe exudates.

Radulescu et al [10], attained unique properties of various antimicrobial textiles beneficial in different skin dermal infections which contained vital oils. They clarified and compared the effect of oils and emulsions on textiles which concluded the antimicrobial activity of emulsions was weaker than the antimicrobial activity of vital oils before and after impregnation on textiles. Sadeghi et al [11], studied the polymeric films to sustain the drug release capacity of the ocular inserts by using sodium alginate polymer and enriching the antibacterial activity by using the Linezolid drug. They concluded the alginate copolymer exhibited sustained release ability.

In this study, bio-films comprising sodium carboxymethyl cellulose, sodium alginate, and unification of them with Tween(80) were utilized effectively as wound dressing stimulus. Sodium carboxymethylcellulose, sodium alginate, and Tween(80) were selected due to their favorable properties that were mentioned earlier. Additionally, by blending sodium carboxymethyl cellulose/sodium alginate, the authors aimed to intent the attributes of the bio-polymeric infrastructure. Nevertheless, this was not realized. Forthcoming, Tween(80) was added to enrich the mucoadhesiveness of the bio-film system considering it is willful to be utilized in the dermal bandages. Linezolid antibiotic was padded to ameliorate the antimicrobial aptitude of the refined films. Eventually, this work will intend to attend a unique wound bandage strategy with refined antipathogenic and wound recuperation to avert intense wound infection which can point to outcast effects for instance bacteremia and multitudinous organ dub.

2. Detailed Experimental Work

2.1. Materials used

Carboxymethyl cellulose (sodium salt) known as (carmellose sodium) which purity percentage is represented about (99.5%) of Na-CMC and mixtures (0.5%) salt (sodium chloride, sodium glycolate) in

addition to the percentage of viscosity about (1% aq. at 25° C) 4000–5000 cP, physical state (solid), colour (white powder), pH (6.5–8.5), density (1.59 g/cm^3), solubility (soluble in water) and loss on drying (max. 10%). Carmellose sodium was obtained from a (German Company, Lanxess, Engineering Chemistry). Sodium alginate (Na-Alg) was purchased from (Carlroth Co.). Tween(80) has chemical formula [($C_{62}H_{122}O_{26}$) and D = 1.09 g/cm^3] was purchased from Scharlau Chemie S.A. Linezolid (LZD) is a synthetic antibacterial agent of the oxazolidinone class which the chemical name for linezolid is (S)-N-[[3-[3-Fluoro-4-(4morpholinyl)phenyl]-2-oxo-5-oxazolidinyl] methyl]-acetamide of chemical formula [($C_{16}H_{20}FN_3O_4$)] and MW (337.35 g/mol) was purchased from Pharmaceutical Chemicals, Egypt.

2.2. Sample preparation method

2.2.1 Preparation of binary films with the specific content of (Tween (80)) solution and different concentrations of the model drug (Linezolid)

Certain amounts of sodium carboxymethyl cellulose and sodium alginate (Na-CMC/Na-Alg) solution were prepared with a specific amount of surfactant (Tween(80)). The solution of (Na-CMC/Na-Alg) was divided into 4 beakers then surfactants were dropped through a pipette with specific amounts and dropped Linezolid drug by using a medical syringe with various amounts. All samples were poured onto clean plastic Petri plates and dried in incubation at 50°C for 6 days. Figure (1**)** exhibits the steps of a mechanism used for the prepared mixture and **Table (1)** presents the compositions of the biofilm samples.

Table (1): Samples with different amounts of the model drug.

No.	(Na-CMC/Na-Alg) (ml)	Surfactant (Tween(80)) (ml)	Drug (Linezolid) (LZD) (mg/g)
1	50/50	0.1 ml (Tween(80))	20 mg/g (Linezolid)
2	50/50	0.1 ml (Tween(80))	40 mg/g (Linezolid)
3	50/50	0.1 ml (Tween(80))	60 mg/g (Linezolid)
4	50/50	0.1 ml (Tween(80))	80 mg/g (Linezolid)

2.3. Characterization of studied films

2.3.1. Physicochemical characterization

- To investigate the dispersion state of antibiotic drugs within the biofilm samples and their outcome on the amorphosity percentage of the polymer components, XRD analysis of blend/Tween(80) and the blend/Tween(80)/linezolid drug samples was carried out using X-ray diffractometer (PAN analytical X` Pert PRO XRD system) with CuKα radiation (λ = 1.540 Å) at 30 kV. Data were obtained in the range of 5 to 80°C at STP.
- Interactions between polymers and drugs were examined by using an FTIR spectrophotometer (Nicolet is 10 single beam FT-IR spectrometer) with KBr pellets route. The spectra study regions were

from 4000 to 400 cm^{-1}.

- The optical properties of the samples were detected by using a UV/vis spectroscopy (JASCO Corp, V-570, Rel. 60–640) double-beam spectrometer. The spectra study regions were from 190 to 2500 nm.
- Morphology of the cross-section of the samples was inspected by using the SEM technique (JEOL JSM-6510LV, USA). The bio-film samples were prepared by the drying method to retain their form and factual component structure. The microphotographs were possessed within a magnification of (2000 ×).

2.3.2. Antimicrobial evaluation study

The antimicrobial activity of the wound bandage was assessed by an inhibition zone approach. Four pathogenic bacteria and one fungus comprising Gram-negative (*E. coli*, *P. aeruginosa*), Gram-positive (*S. aureus*, *B. subtilis*), and fungus (*C. albicans*) were employed for the trial of the dressing antimicrobial activity. Briefly, a dressing disc with a specific diameter was dipped in 1 mg/ml DMSO with fixed shaking. Then the wound dressing disc was incubated, taken out, and washed with sterile water twice times [12].

3. Result And Discussion

3.1. X-ray diffraction scans (XRD)

Generally, XRD analysis is a non-destructive technique utilized to scrutinize the crystallinity, amorphicity, and physical nature of the tested samples. Figure (2**)** depicts the XRD of the Linezolid drug alone which submitted sharp intense peaks at θ scattering angles at **Table (2)** confirming the nature crystallinity of the drug [13, 14]. But when Linezolid was incorporated into the polymer blend/ (0.1 ml) Tween(80), the interaction between the high content of Linezolid drug especially 40, 60, and 80 mg/g, and the blend do not hinder crystal peaks of Linezolid drug **Fig. (2)**. The explanation of this case may be, that because of dilution with a solution of polymer/surfactant, there is no significant change in d-spacing values implying no change in the crystal form of the drug but the crystal habit of the drug might be changed thus suggesting the absence of a polymorphic transition. Or maybe due to the Linezolid drug represented (I) form that is the most common crystalline form, also due to the high content of Linezolid drug which not diluted completely in mixture solvent [15, 16].

Table (2): The most important reflections and their relative intensities of the Linezolid drug.

2θ°	I%
14.46°	21.37
17.02°	33.54
19.5°	36.52
20.5°	19.96
28.22°	36.52

3.2. Fourier transforms infrared analysis (FTIR)

The molecular structure of (Linezolid drug), (Blend/(0.1ml) Tween (80)/(20mg/g) Linezolid), (Blend/(0.1ml) Tween(80)/(40mg/g) Linezolid), (Blend/(0.1ml) Tween(80)/(60mg/g) Linezolid) and (Blend/(0.1ml) Tween(80)/(80mg/g) Linezolid) were inspected using FTIR spectroscopy in the spectral range from 400 to 4000 cm^{-1}, and the results are demonstrated in **Fig. (3)** and summarized **Table (3)**.

The FTIR absorption spectra of Linezolid can be divided into four major regions: the first region can be seen from 3400 – 3100 cm^{-1} for –NH stretching vibrations; the second region is formed by –CH stretching seen from 3000 – 2820 cm^{-1}, the third region reveals the presence of = CO stretching which can be noticed at the wavenumber region of 1885 – 1700 cm^{-1}, and the fourth region between 1650 – 1550 cm^{-1} assigned to –NH bending and = CO stretching of an acetamide carbonyl [17, 18].

It is known that the absorption bands of (Blend/(0.1 ml) Tween(80)) are observed in the previous system. Therefore, the FTIR spectra of (Blend/(0.1 ml) Tween(80)) after adding different amounts of (Linezolid drug) displayed specific bands for the drug within the investigation region between 4000 – 400 cm^{-1} as shown in **Fig. (3)**. Moving to the FTIR of (Blend/(0.1 ml) Tween(80)/ (20,40,60 and 80 mg/g) Linezolid drug), it is spotted that there are additional peaks are appeared. For instance, the formed peak at 3087 cm^{-1} which could be related to the stretching modes of –NH, band at 2074 cm^{-1} is appointed for –CH stretching, peak at 1743 cm^{-1} appointed for = CO stretching of an acetamide carbonyl, and band at 1648 cm^{-1} ordained for –NH bending (ester and amide bands) and = CO stretching of an oxazolidinone carbonyl. Based on these witnessed peaks, the spectrum reveals that Linezolid drug functionalized (Blend/ 0.1ml Tween(80)) was effectively incorporated [18, 19].

Table (4): Standard and observed wavenumbers of Linezolid drug.

Functional group	Standard frequency (cm^{-1})	Observed frequency (cm^{-1})
N-H Stretching	3100–3400	3115
C-H stretching	2820–3000	2885
C = O stretching	1700–1885	1885
N-H bending and C = O stretching	1550–1650	1648

3.3. Ultraviolet and visible analysis (UV/Vis.) studies

The UV/Vis scan of standard Linezolid between (190–1100) nm showed the absorption maxima at (219.5 and 281.2) nm, shown in **Fig. (4)** [20, 21]. The two absorption bands display a peak which is referred to as π-π* transition referring to the transition from the valence band to the conduction state, linked to the extent of conjunction along the drug chain such as = CO stretching of an oxazolidinone carbonyl at (1746 cm^{-1}) and = CO stretching of an acetamide carbonyl at (1447 cm^{-1}) according to band assignments in FTIR spectra.

Consequently, its extinction coefficients for wavelengths are still less than (250) nm, after adding different contents of Linezolid drug to the (blend/surfactant) matrix due to its transparency as shown in **Fig. (4)**. The reaction between blend/surfactant and Linezolid showed a wide band and disappearance of = CO stretching at (1735 cm^{-1}) in Tween(80) absorption bands due to the split and the building again of these bonds that can be proved by altering the crystallinity and enhancing the stabilization efficiency of the formed blend/surfactant/Linezolid. Optical energy gaps variation of the spectra indicates the complexation and the miscibility between the drug and blend/surfactant matrix [22].

3.3.1. Absorption coefficient and band gap studies

Figure (5) showed the relationship between α versus photon energy for the Linezolid drug. Interestingly, it is seen that the absorption edge value at 4.43 and 5.57 eV for the pure drug. The absorption coefficients (α) can be estimated by Beer-Lambert's formula [23, 24]:

$$\alpha(\lambda) = \frac{2.303\,A}{d} \qquad (1)$$

Where **A** and **d** represent the absorbance and the film's thickness, respectively.

The transformation form is shown by the power (m), which becomes direct at **m = 0.5** and indirect at **m = 2**, as seen in **Table (5)**. Both direct and indirect band gaps of drugs behave similarly, even though the indirect has a higher value than the direction as in **Fig. (10(a-b))**. In addition, the bandgap can be calculated as [23, 25]:

$$\alpha h\nu = A\,(h\nu - E_g)^m \qquad (2)$$

Where (**hv**) refers to the photon energy, E_g represents the bandgap and **A** is the band tailing parameter.

The absorption coefficient (α) as a function of incident energy of (Blend/(0.1 ml) Tween(80)) and (Blend/(0.1 ml) Tween(80)/ (20,40,60 and 80 mg/g) Linezolid drug) films was depicted in **Fig. (6)**. The coefficient (α) value is significantly affected by Linezolid drug content. Because of the complex fundamental interaction between the blend/surfactant matrix and the Linezolid drug which appeared in blend/surfactant matrix/different content of Linezolid drug rather than blend/surfactant matrix. Also, the absorption edges decline from 4.06 eV for blend/surfactant to 1.78 eV for the high content of linezolid drug in blend/surfactant matrix.

The values of band gaps decreased dramatically after the addition of different contents of Linezolid drug to the blend/ (0.1ml) Tween(80) as listed in **Table (5)**. The decrease in band gap from (4.8 eV to 3.7 eV) for direct transition and from (5.09 eV to 3.9 eV) for indirect transition after added drug to blend/surfactant may be explained as shown in **Fig. (7(a-b))**. This falling due to the formation of some defects in band gap through the films related to the Linezolid drug addition and also the increase in conjugation also leads to a decrease in the optical band gap. The difference between the optical band gap and the electronic band gap (activation energy) is due to the indirect transition in the system during optical analysis. So, the smaller the band gap, the more electrically conducting material will be [26].

3.3.2. Refractive index study

Upon the addition of the drug, the refractive index increased for blend/Tween(80) which the index of refraction depended on both density and polarizability as shown in **Table (5)**. Furthermore, using the Dimitrov and Sakka equations, the refractive index (n) can be calculated as follow:

$$\frac{n^2-1}{n^2+1} = 1 - \sqrt{\frac{E_g^{in}}{20}} \qquad (3)$$

The calculated refractive index by using the Dimitrov and Sakka equations is enhanced in the blend/surfactant matrix by adding a Linezolid drug and increasing gradually with concentration. This behavior was spotted by Ravindra et al. [27].

3.3.3. Urbach energy measurement (E_U)

Figure (8) showed the relationship between ln(α) versus photon energy for the Linezolid drug. Interestingly, it is seen the value (3.84 eV) for the pure drug.

The variation of ln (α) versus hυ for the films after added Linezolid drug confirmed the decrease of Urbach energy values which is shown in **Figure (9)**, and its values are listed in **Table (5)**. The optical activation energy or called Urbach energy (E_U) can be estimated using the following equation [28]:

$$\alpha(h\nu) = \alpha_{\circ} exp\left(\frac{h\nu}{E_U}\right) \qquad (4)$$

Where (αo) is a constant and (EU) is the Urbach energy.

Urbach energy (E_U) decreases with increasing Linezolid drug content. This drop is due to the growth of the blend/surfactant matrix disorder taken place by the drug. Otherwise, the accruing of the Linezolid drug provides rise to a restructuring of states from band to tail.

Table (5): The activation energy (E_{opt}), energy gap [E_g^d and E_g^{in}], and other calculated optical parameters for the prepared samples.

Samples	E_{opt}	E_g^d	E_g^{in}	A	U	n
Linezolid	3.91	4.23	4.6	4.07	3.84	1.79
(20mg/g) Linezolid	3.4	3.78	3.92	3.83	3.78	1.91
(40mg/g) Linezolid	3.38	3.65	3.9	3.8	3.64	1.96
(60mg/g) Linezolid	3.339	3.65	3.9	3.79	3.64	1.97
(80mg/g) Linezolid	3.4	3.54	3.9	3.8	3.5	1.95

The values of the band gap energies (E_{opt}), (E_g^d), and (E_g^{in}) notice the alteration from high to low by different drug content which confirms the XRD results as shown in **Fig. (10)**. This indicates that the E_{opt} is essentially affected by the crystalline structure. This indicates that the linezolid addition significantly influences the energy gap by producing cross-linking within the blend. This denotes a well-defined π-π* transition associated with the formation of conjugated electronic structure between the polymer blend/ surfactant and drug.

3.4. Scanning Electron Microscopy (SEM)

For a description of the morphological building, SEM was performed at magnification (2000x) and later implemented in **Fig. (11(a-d))**. Figure (1**1(a))** verifies the scanned pure drug surface in crystal needlelike (Kadam et al (2017)) [29]. For all tested samples in **Fig. (11(b-d))**, a porous, and coarseness structure with obvious edges is observed. On account of the congeniality between the reactants, both the existence of roughness, pores structures prop competence drug loading. Beyond, the (Linezolid) chain is efficiently conjoined to (Blend/(0.1ml) Tween(80)) as a biopolymer, or the morphology was incited by the drug chemical composition [30].

3.4.1. Surface Roughness

Gwyddion software was used to compute the data of the topography illustrations that were verified in **Table (6)**. Figure (1**1(b-d))** depicts assorted peaks that signify the rough and porous morphology of the

samples after adding the Linezolid drug. The considerable peaks point to the highest coarseness. From these results, the motives of drug release are initially directed to some extent by surface phenomena. Therefore, adjusting surface roughness can direct by the sustained drug release which is described by Van de Belt et al [31]. The surface roughness parameters values for all analyzed samples are presented in **Table (6)** and a detailed explanation of these parameters is collected in **Table (7)** [32]. Figure (1**2)** indicates the increase in surface roughness with the addition of drug content. It was clear that surface morphology was dependent on the complex content and the variation in drug content.

Table (6): Estimated roughness data for all analyzed samples.

Specimen	Blend/(0.1ml) Tween(80)/(20mg/g) Linezolid	Blend/(0.1ml) Tween(80)/(60mg/g) Linezolid	Blend/(0.1ml) Tween(80)/(80mg/g) Linezolid
R_a	45.9565	56.2349	56.2349
R_q	77.1717	89.3332	89.3332
R_t	889.892	939.142	939.142
R_v	273.056	359.981	359.981
R_p	616.837	579.161	579.161
R_z	671.981	767.372	767.372
$R_{y=}R_{max}$	889.892	845.320	845.320
W_a	51.1344	60.5617	60.5617
W_q	73.3275	80.4826	80.4826
$W_{y=Wmax}$	447.309	504.600	504.600
P_t	973.449	999.153	999.153

Table (7): Surface roughness parameters.

Parameter	Name	Illustrative graph
R_a	Average roughness	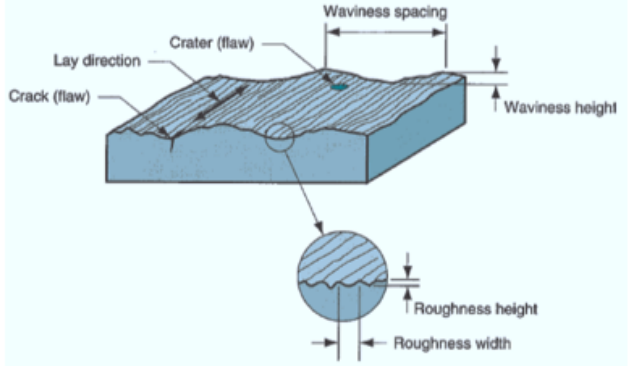
R_q	Root mean square roughness	
R_t	Maximum height of the roughness	
R_v	Maximum roughness valley depth	
R_p	Maximum roughness peak height	
R_z	Average maximum height of the profile	
W_a	Waviness average	
W_q	Root mean square waviness	
$W_{y=Wmax}$	Waviness maximum height	
P_t	Maximum height of the profile	

3.5. Antibacterial analysis

The antimicrobial efficacy of blend/(0.1ml) Tween(80)/(20, 40, 60 an,d 80mg/g Linezolid) as a wound dressing antibiotic was inspected using several distinct species of germs and fungus such as *E.coli*, *P.aeuroginosa, S.aureus*, *B.subtilis*, and *C.albicans* as well. The evaluation was estimated via determining the inhibition zone diameter (mm) and activity index (%) of the killed microbes and fungus due to the antimicrobial effect of Linezolid after submission of the designated complex for study and the attained data are delineated in **Table (8)** and **Fig. (13(a-e))** [3, 4]. It has been observed that the efficacy of the combination of blend/(0.1ml) Tween(80)/ Linezolid for killing or averting the microbes and fungus diffusion which means that *C.albicans* for sample (3) *is* more sensitive than the other tested microbes towards the effect of Linezolid. While the other samples enrolled finer antimicrobial attributes concerning all tested microbes and fungus rather than antimicrobial properties of blend/(0.1ml) Tween(80). The greater outcome for the last blend/surfactant/drug could be assigned to the large surface area which enriches the plain invasion of the drug inside the tested microbes and fungus walls. Based on the above-mentioned outcomes, it can be inferred that the antimicrobial features of blend/(0.1ml) Tween(80)/Linezolid drug are greater than that of blend/(0.1ml) Tween(80) compounds. For illustration, a graphic representation of the activity index (%) is shown in **Figure (14(a-e))**. The % activity index for the tested samples was measured by the below formula [33, 34]:

$$\%\ Activity\ Inde = \frac{Zone\ of\ inhibition\ by\ test\ compound\ (diametre)}{Zone\ of\ inhibition\ by\ standard\ (diametre)}\ x\ 100 \qquad (5)$$

Table (8): Antimicrobial activity of (blend/Tween(80) surfactant/ different content of linezolid drug) against different bacterial and fungi.

Compound	*E. coli*		*Pseudomonas aeuroginosa*		*S. aureus*		*Bacillus subtilis*		*C. Albicans*	
	D (mm)	A (%)	D (mm)	A (%)	D (mm))	A (%)	D (mm)	A (%)	D (mm)	A (%)
1	**3**	**11.5**	**4**	**17.4**	**2**	**8.3**	**6**	**26.1**	**7**	**25.9**
2	**10**	**38.5**	**9**	**39.1**	**6**	**25.0**	**11**	**47.8**	**8**	**29.6**
3	**8**	**30.8**	**12**	**52.2**	**8**	**33.3**	**8**	**34.8**	**14**	**51.8**
4	**5**	**19.2**	**7**	**30.4**	**9**	**37.5**	**10**	**43.5**	**10**	**37.0**
Ampicillin	**26**	**100**	**23**	**100**	**24**	**100**	**23**	**100**	—	—
Clotrimazole	—	—	—	—	—	—	—	—	**27**	**100**
D (mm) is the diameter of the inhibition zone, and **A (%)** is the Activity index.										

- **Clarification of samples numbers.**

1	**Blend/(0.1ml) Tween(80)/20mg/g linezolid**
2	Blend/(0.1ml) Tween(80)/40mg/g linezolid
3	Blend/(0.1ml) Tween(80)/60mg/g linezolid
4	Blend/(0.1ml) Tween(80)/80mg/g linezolid

4. Conclusions

The attained data verify the use of polymers, surfactants, and antimicrobial agents in the expansion of innovative bandages that could furnish relevant clinical prospects in the wound cure domain. XRD data demonstrated the intensities of the peaks decreased to some extent due to the decreased crystallinity of the linezolid drug in matrices. FTIR data depicted the interactions between Linezolid and polymer matrices. UV/Vis data indicated the complexation and the miscibility between the drug and blend/surfactant matrix. Further, the morphology of the films observed the porous, and coarseness structure with plain edges. The in vitro antibacterial assay of bio-films formulations was assessed in bacterial and fungal strains, showing a significant activity over time. In conclusion, the Na-CMC/Na-Alg blend with Tween(80) and Linezolid drug developed in this study manifested appropriate physicochemical, optical, and antimicrobial properties to be applied as a wound dressing with refined antipathogenic and wound recuperation to avert intense wound infection which can point to outcast effects for instance bacteremia and multitudinous organ dub.

References

1. S. Hu, X. Cai, X. Qu, B. Yu, C. Yan, J. Yang, X. Shi, Preparation of biocompatible wound dressings with long-term antimicrobial activity through covalent bonding of antibiotic agents to natural polymers. International journal of biological macromolecules 123 **(2019)** 1320-1330.
2. S. Sharma, B. Sharma, S. Shekhar, P. Jain, Natural Polymer-Based Composite Wound Dressings, In Polymeric and Natural Composites, Springer, Cham **(2022)** 401-423.
3. A.A. Novikova, V.V. Zavarzina, E.A. Vorontcov, S.E. Severin, Preparation of polymeric composition of linezolid and study of its antimicrobial activity in vitro, Nanotechnologies in Russia 9(7) **(2014)** 453-456.
4. G. Carreño, A.Marican, S. Vijayakumar, O. Valdés, G. Cabrera-Barjas, J. Castaño, E.F. Durán-Lara, Sustained release of linezolid from prepared hydrogels with polyvinyl alcohol and aliphatic dicarboxylic acids of variable chain lengths, Pharmaceutics 12(10) **(2020)** 982.
5. G. Singh, M.W. Khan, A. Patel, Formulation and Biological Implication of Eucalyptus Globulus and Trachspermum ammi Organogel for Topical Delivery, Reviews in Pharmacy and Pharmaceutical Sciences 1(1) **(2022)** 1-4.
6. T. Maver, L. Gradišnik, D.M. Smrke, K. Stana Kleinschek, U. Maver, Systematic evaluation of a diclofenac-loaded carboxymethyl cellulose-based wound dressing and its release performance with changing pH and temperature, AAPS PharmSciTech 20(1), **(2019)** 1-12.
7. B. Jadach, W. Świetlik, A. Froelich, Sodium alginate as a pharmaceutical excipient: novel applications of a well-known polymer, Journal of Pharmaceutical Sciences **(2022)**.
8. F. Rancan, J. Jurisch, C. Günday, E. Türeli, U. Blume-Peytavi, A. Vogt, N. Günday-Türeli, Screening of Surfactants for Improved Delivery of Antimicrobials and Poly-Lactic-co-Glycolic Acid Particles in Wound Tissue, Pharmaceutics 13(7) **(2021)** 1093.
9. M. Ali, N.R. Khan, H.M. Basit, S. Mahmood, Physico-chemical based mechanistic insight into surfactant modulated sodium Carboxymethylcellulose film for skin tissue regeneration applications, Journal of Polymer Research 27(1) **(2020)** 1-11.
10. D.E. Radulescu, A. Popescu, A. Danila, L. Chirila, E.I. Muresan, BIOACTIVITY AND DERMAL TOXICITY OF SKIN CARE TEXTILES, International Multidisciplinary Scientific GeoConference: SGEM 19(6.1) **(2019)** 51-59.
11. A.M. Sadeghi, F. Farjadian, S. Alipour, Sustained release of linezolid in ocular insert based on lipophilic modified structure of sodium alginate, Iranian journal of basic medical sciences 24(3) **(2021)** 331.
12. M. Balouiri, M. Sadiki, S.K. Ibnsouda, Methods for in vitro evaluating antimicrobial activity: A review, Journal of pharmaceutical analysis 6(2) **(2016)** 71-79.
13. E.G. Karagiannidou, Solid state characterization of linezolid crystal forms, International Journal of Analytical, Pharmaceutical and Biomedical Sciences 2(2) **(2013)**.

14. A.M. Kadam, S.S. Patil, Improvement of micromeritic, compressibility and solubility characteristics of linezolid by crystallo-co-agglom-eration technique, International Journal of Applied Pharmaceutics 9(4) **(2017)** 47-53.
15. L. Tammaro, C. Saturnino, S. D'Aniello, G. Vigliotta, V. Vittoria, Polymorphic solidification of Linezolid confined in electrospun PCL fibers for controlled release in topical applications, International journal of pharmaceutics 490(1-2) **(2015)** 32-38.
16. B. Darbasizadeh, S.A. Mortazavi, F. Kobarfard, M.R. Jaafari, A. Hashemi, H. Farhadnejad, B. Feyzi-barnaji, Electrospun Doxorubicin-loaded PEO/PCL core/sheath nanofibers for chemopreventive action against breast cancer cells, Journal of Drug Delivery Science and Technology 64 **(2021)**102576.
17. S.K. Khatri, M. Rathnanand, R. Nikhila, Formulation and evaluation of wound healing activity of linezolid topical preparations on diabetic rats, International Journal of Applied Pharmaceutics 8(3) **(2016)** 30-36.
18. T. Eren Boncu, N. Ozdemir, A. Uskudar Guclu, Electrospinning of linezolid loaded PLGA nanofibers: effect of solvents on its spinnability, drug delivery, mechanical properties, and antibacterial activities, Drug development and industrial pharmacy 46(1) **(2020)** 109-121.
19. A.R. Golhar, V.K. Ghume, D.A.N. Merekar, M.D. Dokhe, D.B. Patil, FORMULATION AND EVALUATION OF LIPOSOMAL TOPICAL GEL OF LINEZOLID FOR THE TREATMENT OF SKIN INFECTION **(2020)**.
20. B.H. Saikiran, S.K. Johnny, UV SPECTROSCOPIC METHOD FOR ESTIMATION OF LINEZOLID IN TABLETS, International Journal of Pharmaceutical, Chemical & Biological Sciences 3(3) **(2013)**.
21. S. ElWeshahy, Validated stability indicating assay of linezolid by spectrophotometric and high performance liquid chromatographic methods, Australian Journal Of Basic and Applied Sciences 6(3) **(2012)** 767-778.
22. M. Faisal, M.A. Rashed, J. Ahmed, M. Alsaiari, A.S. Alkorbi, M. Jalalah, F.A. Harraz, Rapid photodegradation of linezolid antibiotic and methylene blue dye over Pt nanoparticles/polypyrrole-carbon black/ZnO novel visible light photocatalyst, Journal of Environmental Chemical Engineering 9(6) **(2021)** 106773.
23. A.A. Menazea, A.M. Mostafa, E.A. Al-Ashkar, Effect of nanostructured metal oxides (CdO, Al_2O_3, Cu_2O) embedded in PVA via Nd: YAG pulsed laser ablation on their optical and structural properties, Journal of Molecular Structure **(2020)** 1203-127374.
24. L. Teodorof, A. Burada, C. Despina, S.O. Daniela, A. Ene, UV-VIS spectroscopic methods for environmental analysis, Common borders. Common solutions. 7 **(2021)**.
25. S.I. El-dek, S.F. Mansour, M.A. Ahmed, M.K. Ahmed, Microstructural features of flower like Fe brushite, Prog. Nat. Sci.: Materials International 27 **(2017)** 520–526.
26. S. Islam, M. Ganaie, S. Ahmad, A. M. Siddiqui, M. Zulfequar, Dopant effect and characterization of poly (o-toluidine)/vanadium pentoxide composites prepared by in situ polymerization process, International Journal of Physics 2 **(2014)** 105–122.

27. V. Gupta, N. Ravindra, Comments on the moss formula, Physica Status Solidi (B) 100 **(1980)** 715–719.
28. S. Awad, S. El-Gamal, A.M. El Sayed, E.E. Abdel-Hady, Characterization, optical, and nanoscale free volume properties of Na-CMC/PAM/CNT nanocomposites, Polym Adv Technol. 31(1) **(2020)** 114-125.
29. A.M. Kadam, S.S. Patil, Improvement of micromeritic, compressibility and solubility characteristics of linezolid by crystallo-co-agglom-eration technique, International Journal of Applied Pharmaceutics 9(4) **(2017)** 47-53.
30. G. Carreño, A. Marican, S. Vijayakumar, O. Valdés, G. Cabrera-Barjas, J. Castaño, E.F. Durán-Lara, Sustained release of linezolid from prepared hydrogels with polyvinyl alcohol and aliphatic dicarboxylic acids of variable chain lengths, Pharmaceutics 12(10) **(2020)** 982.
31. H. Van de Belt, D. Neut, D. Uges, W. Schenk, J. Van Horn, H. Van der Mei, H. Busscher, Surface roughness, porosity and wettability of gentamicin-loaded bone cements and their antibiotic release, Biomaterials 21 **(2000)** 1981–1987.
32. P.M. Santos, E.N. Júlio, A state-of-the-art review on roughness quantification methods for concrete surfaces, Construction and Building Materials 38 (2013) 912-923.
33. D. Dharajiya, P. Patel, M. Patel, N. Moitra, In vitro antimicrobial activity and qualitative phytochemical analysis of Withania somnifera (L.) dunal extracts, International Journal of Pharmaceutical Sciences Review and Research 27(2) **(2014)** 349-354.
34. P. Singariya, P. Kumar, K.K. Mourya, Estimation of Bio-activity of Arial parts of Withania somnifera Against the Bacterial and Fungal Microbes, International Journal of Pharmacy and Pharmaceutical Science, 4(3) **(2012)** 553-557.

Figures

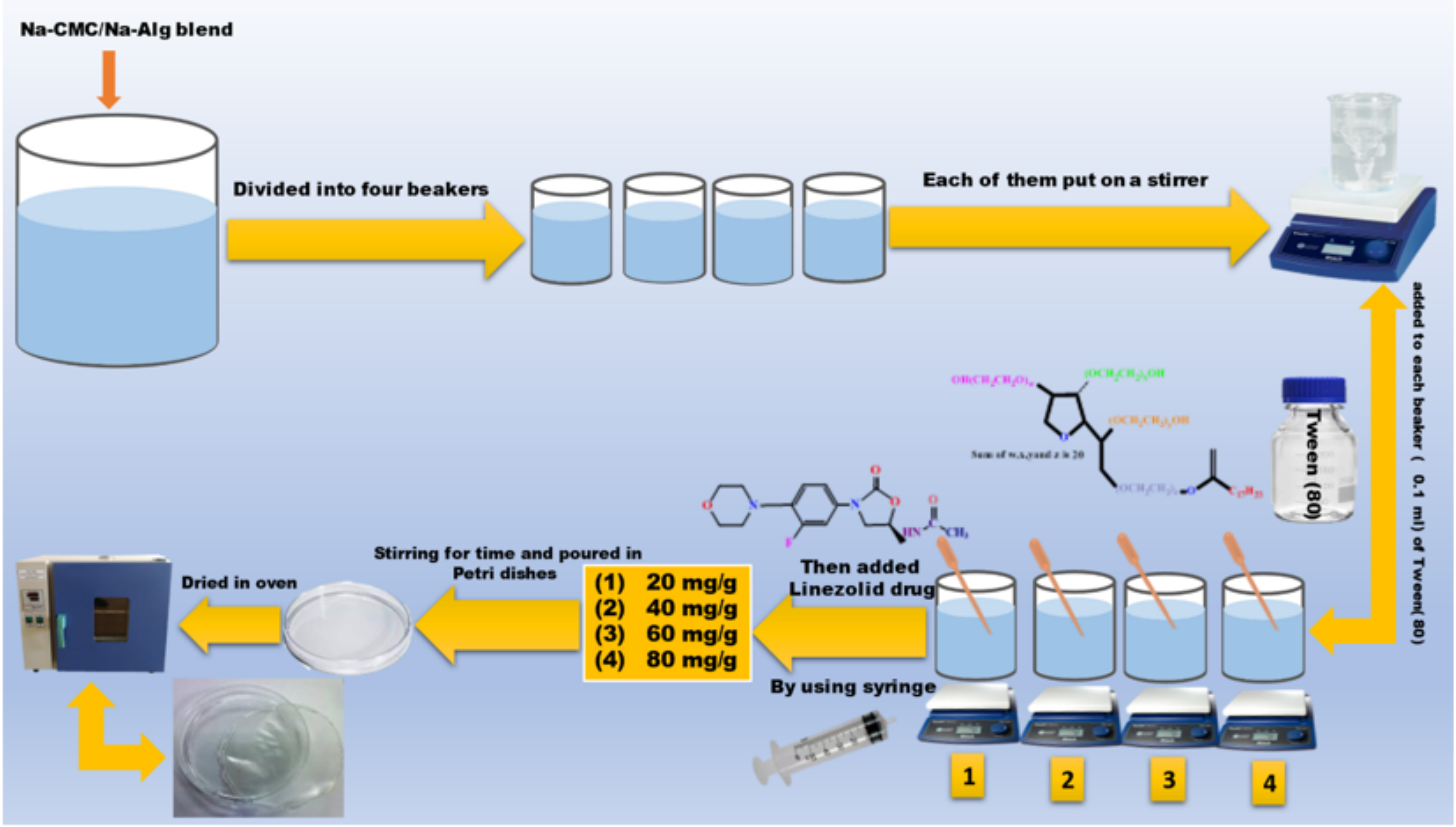

Figure 1

Flow chart of the sample preparation by standard solution cast technique and flexibility of the blend polymer films: preparation of binary solution/ surfactant, and preparation of binary films/ surfactant with different content of Linezolid drug.

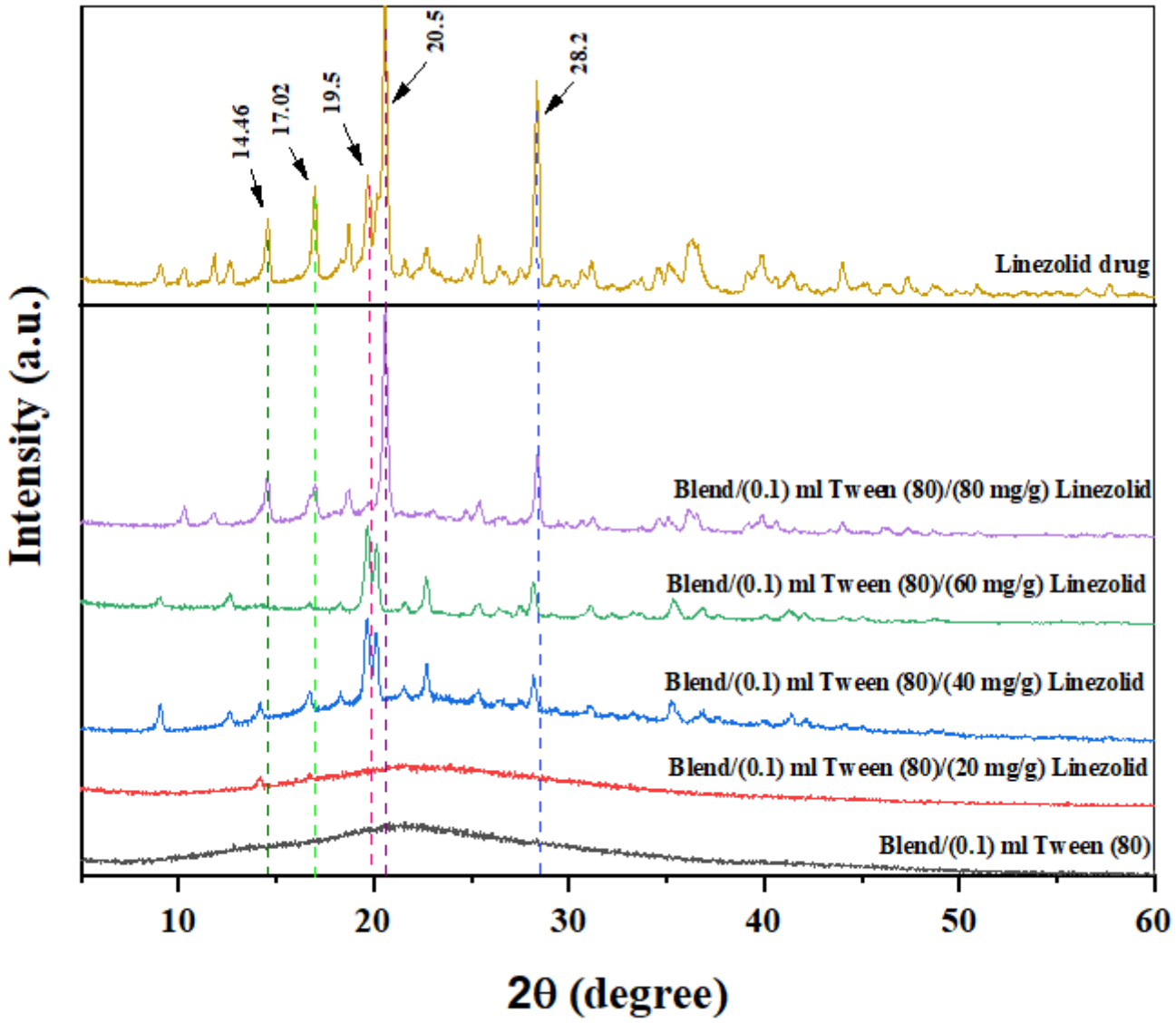

Figure 2

XRD pattern of Blend/(0.1ml) Tween(80)/ different contents of Linezolid drug.

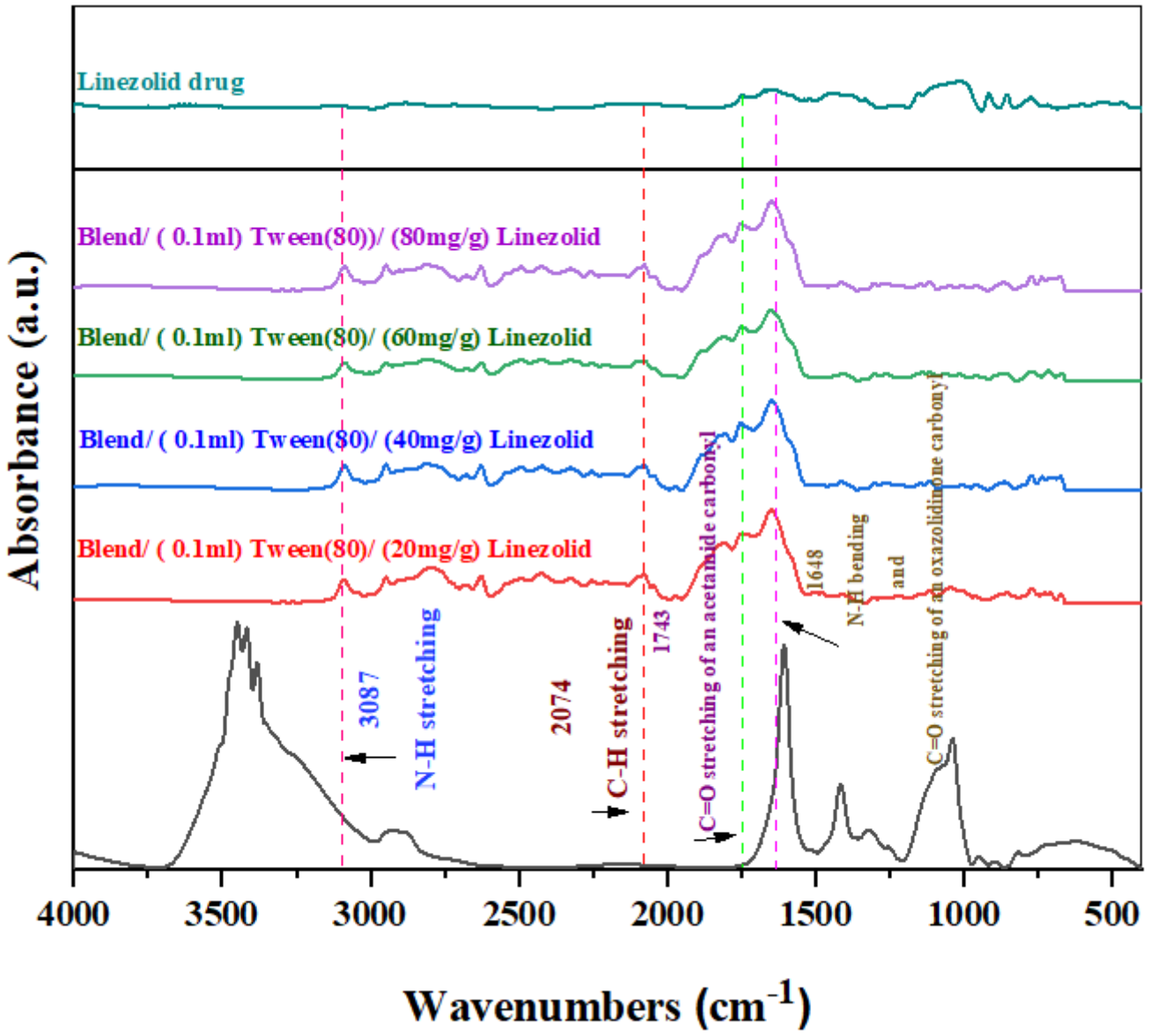

Figure 3

FTIR spectra of Blend/(0.1ml) Tween(80)/ different amounts of Linezolid drug).

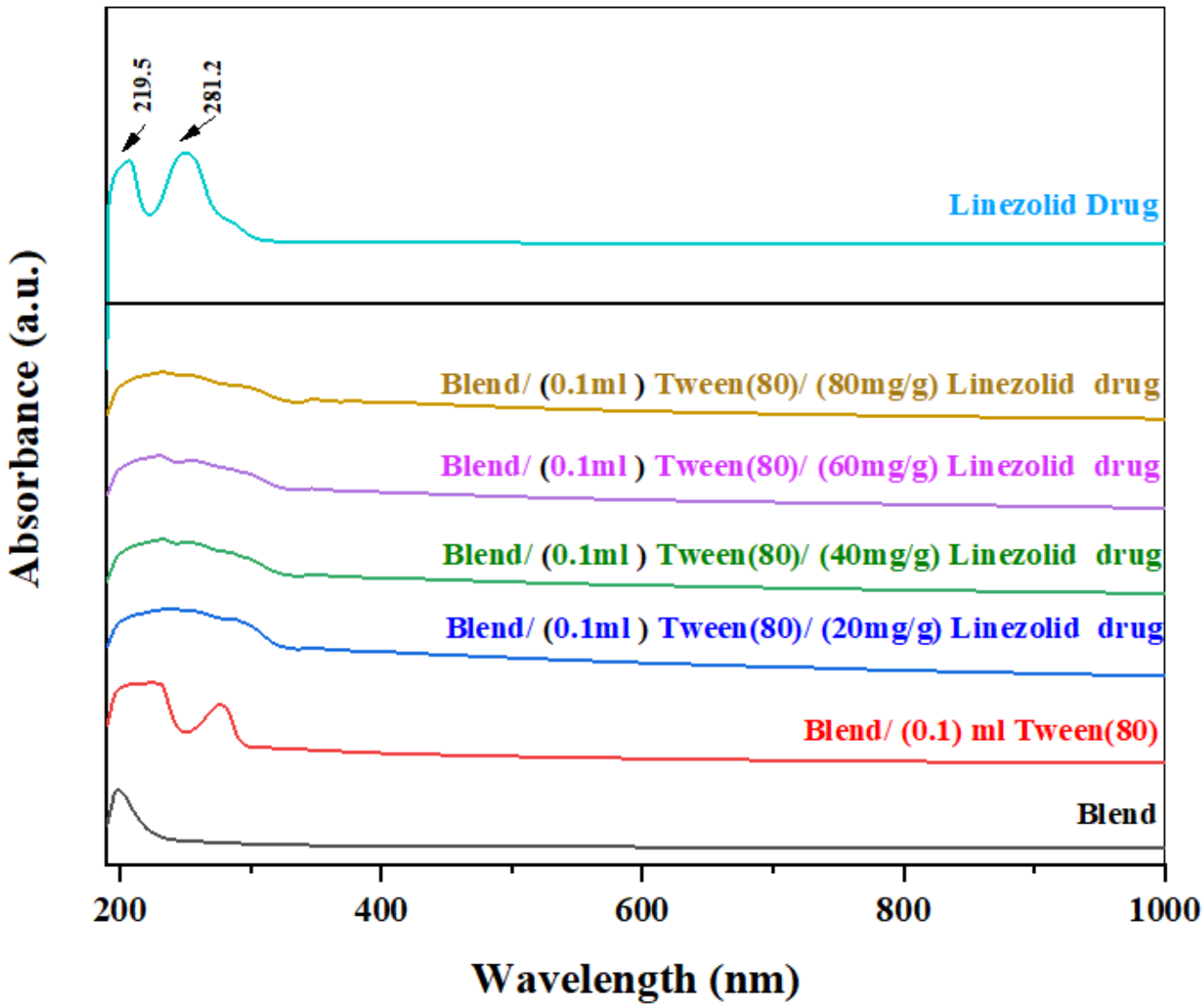

Figure 4

Absorption Spectrum of blend/ (0.1ml) Tween(80)/ different contents of Linezolid drug.

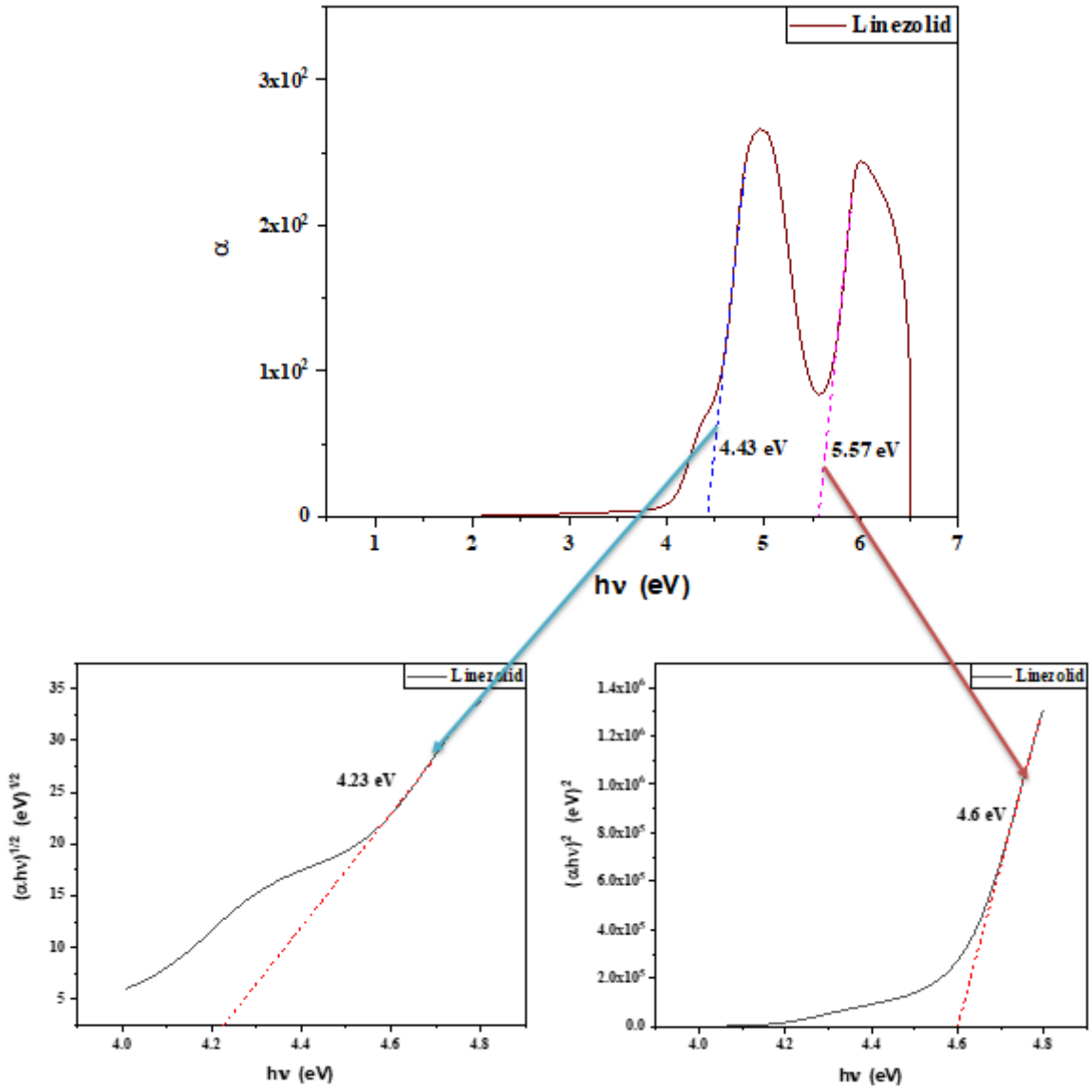

Figure 5

Absorption coefficient, direct and indirect band gaps estimation curve for Linezolid drug.

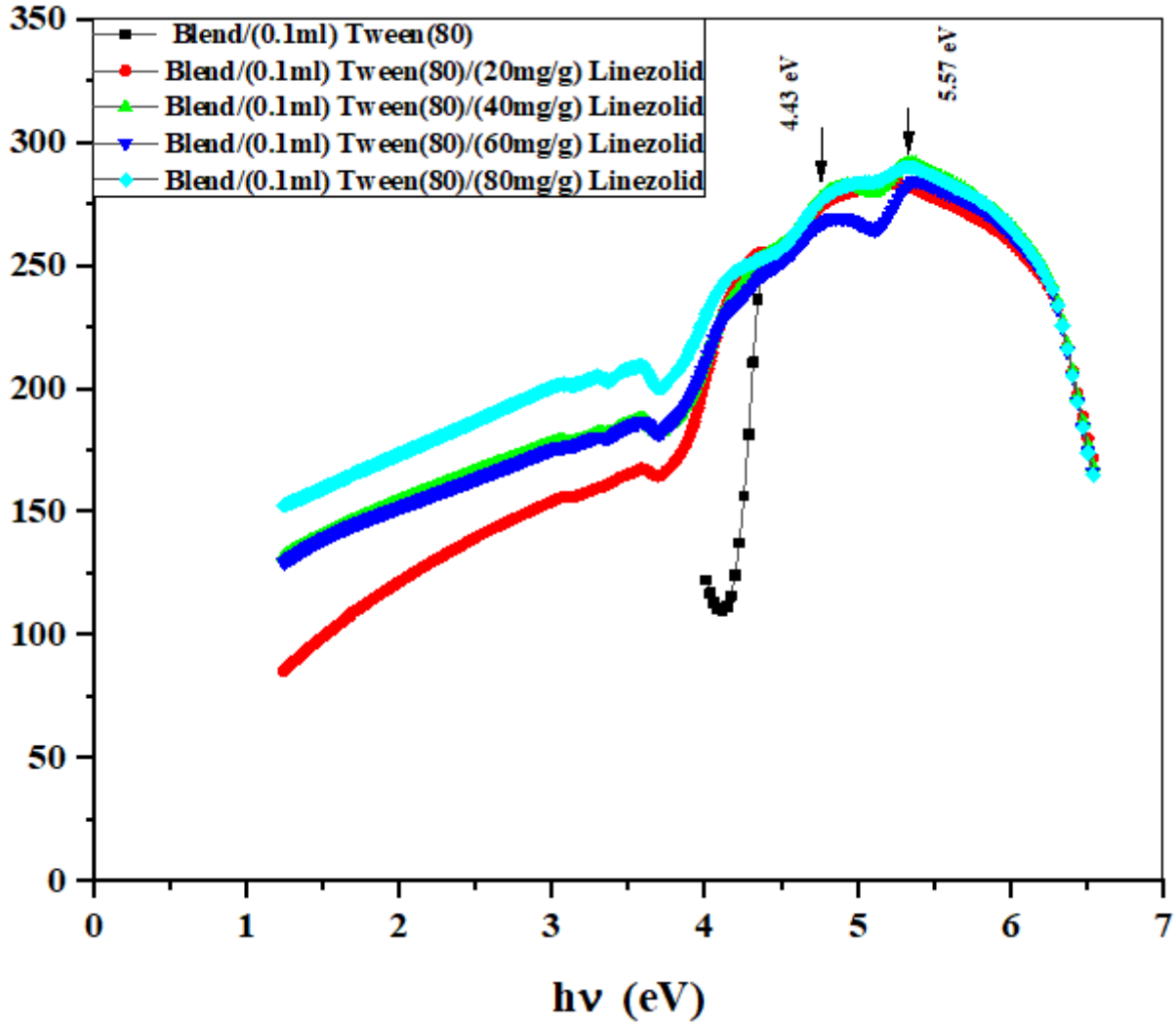

Figure 6

Absorption coefficient of studied samples.

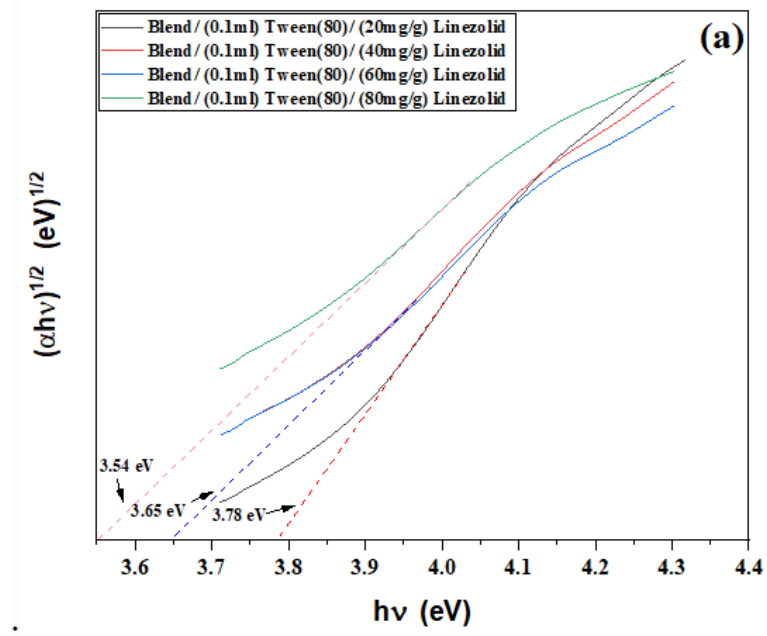

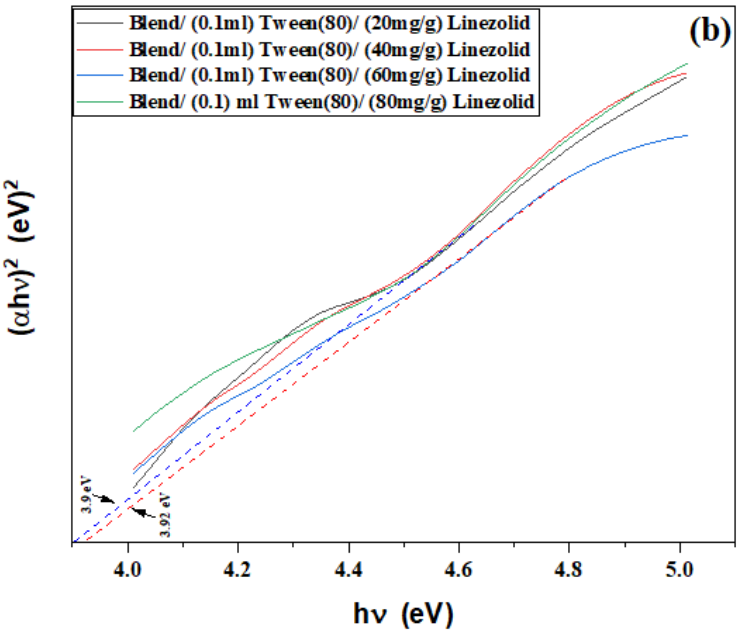

Figure 7

(a-b): Direct and indirect band gaps estimation curve of samples after adding different contents of drug.

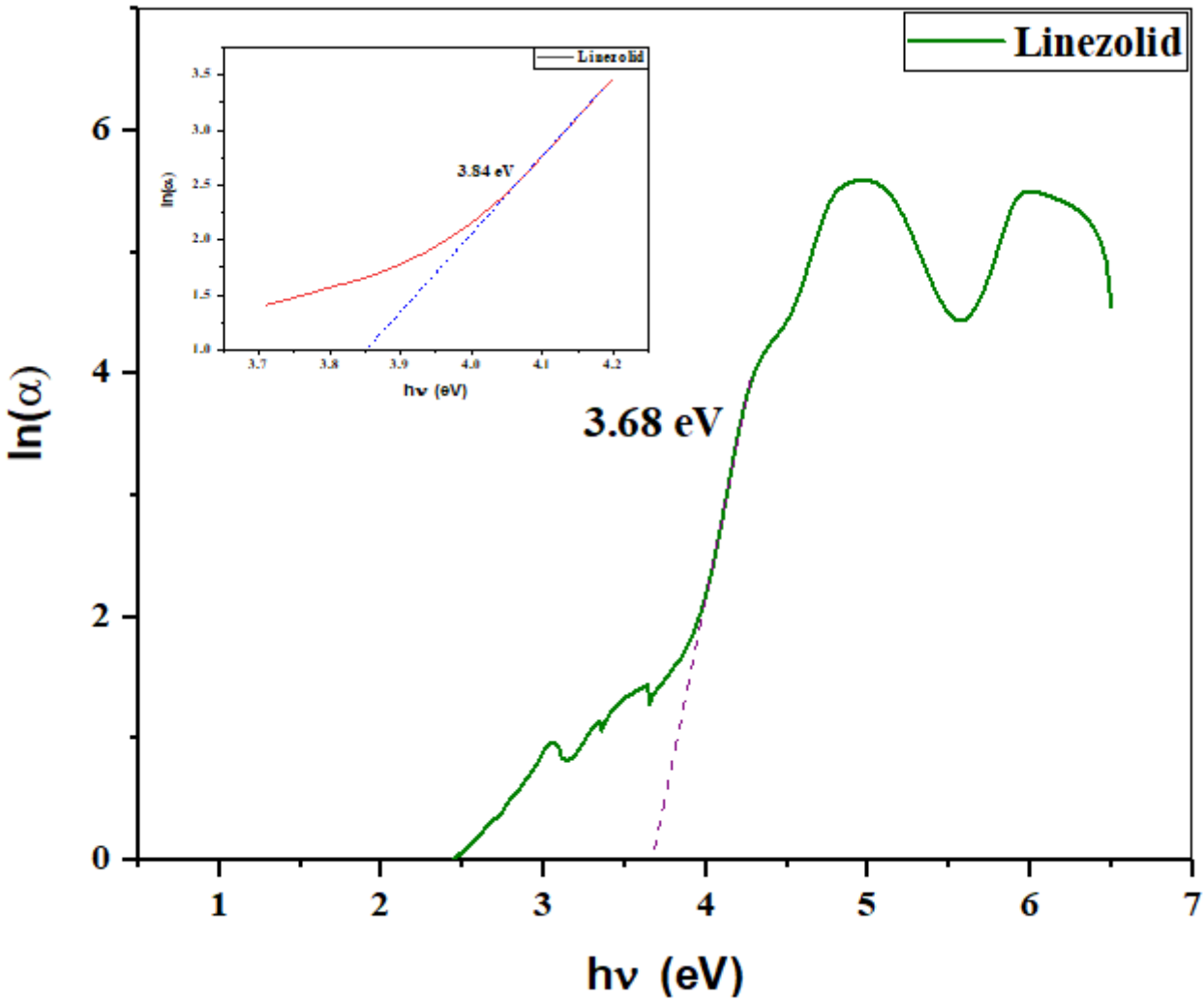

Figure 8

Urbach estimation curve for Linezolid drug.

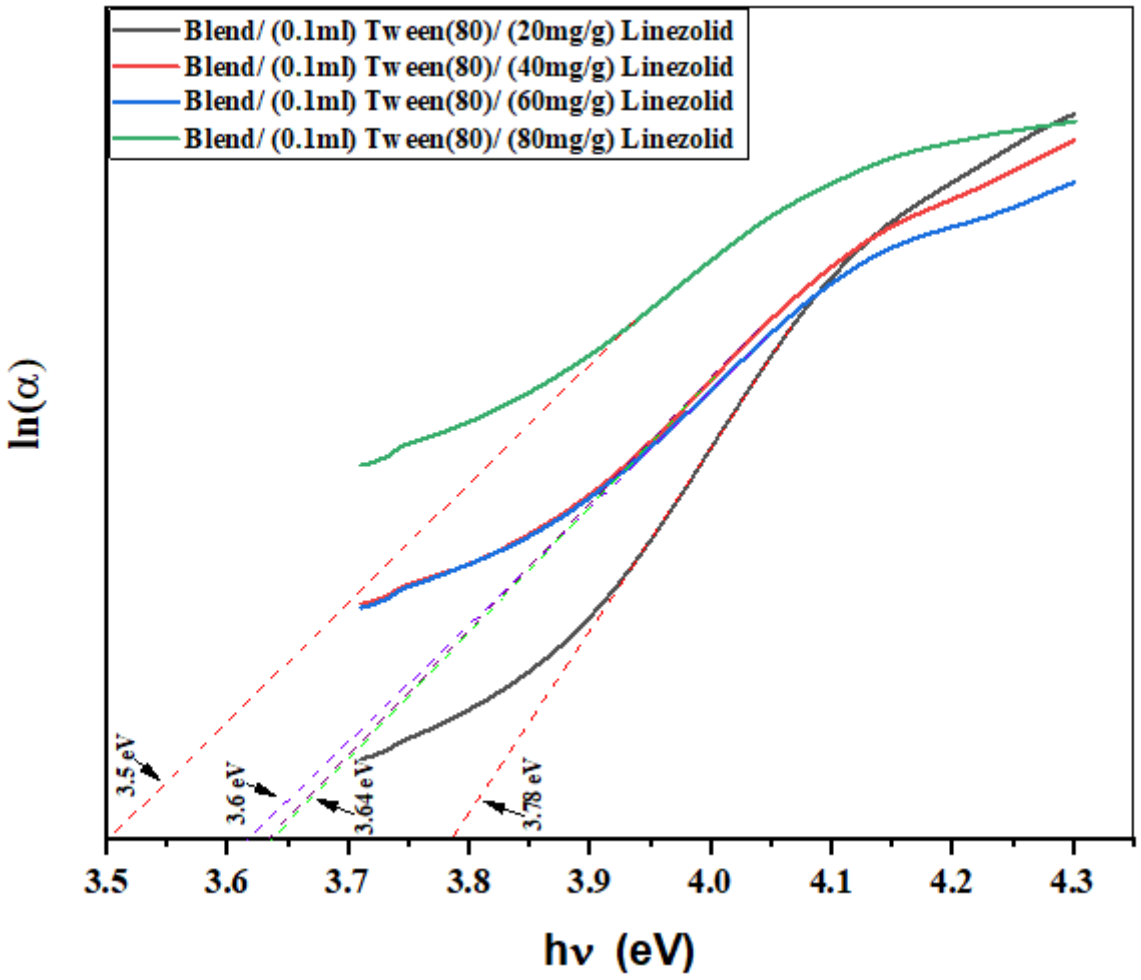

Figure 9

Urbach estimation curve for tested samples after adding different amounts of the drug.

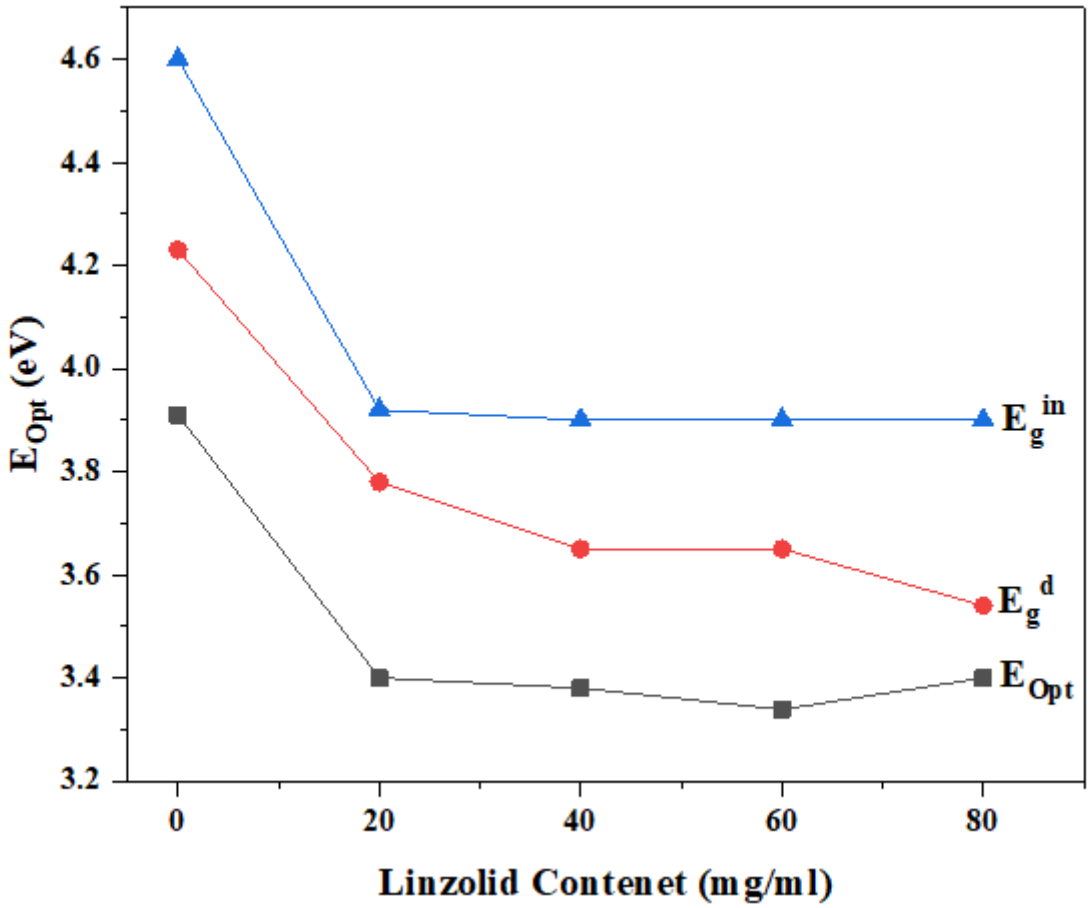

Figure 10

Direct and indirect band gap energies as a function in drug amount in the blend/surfactant matrix.

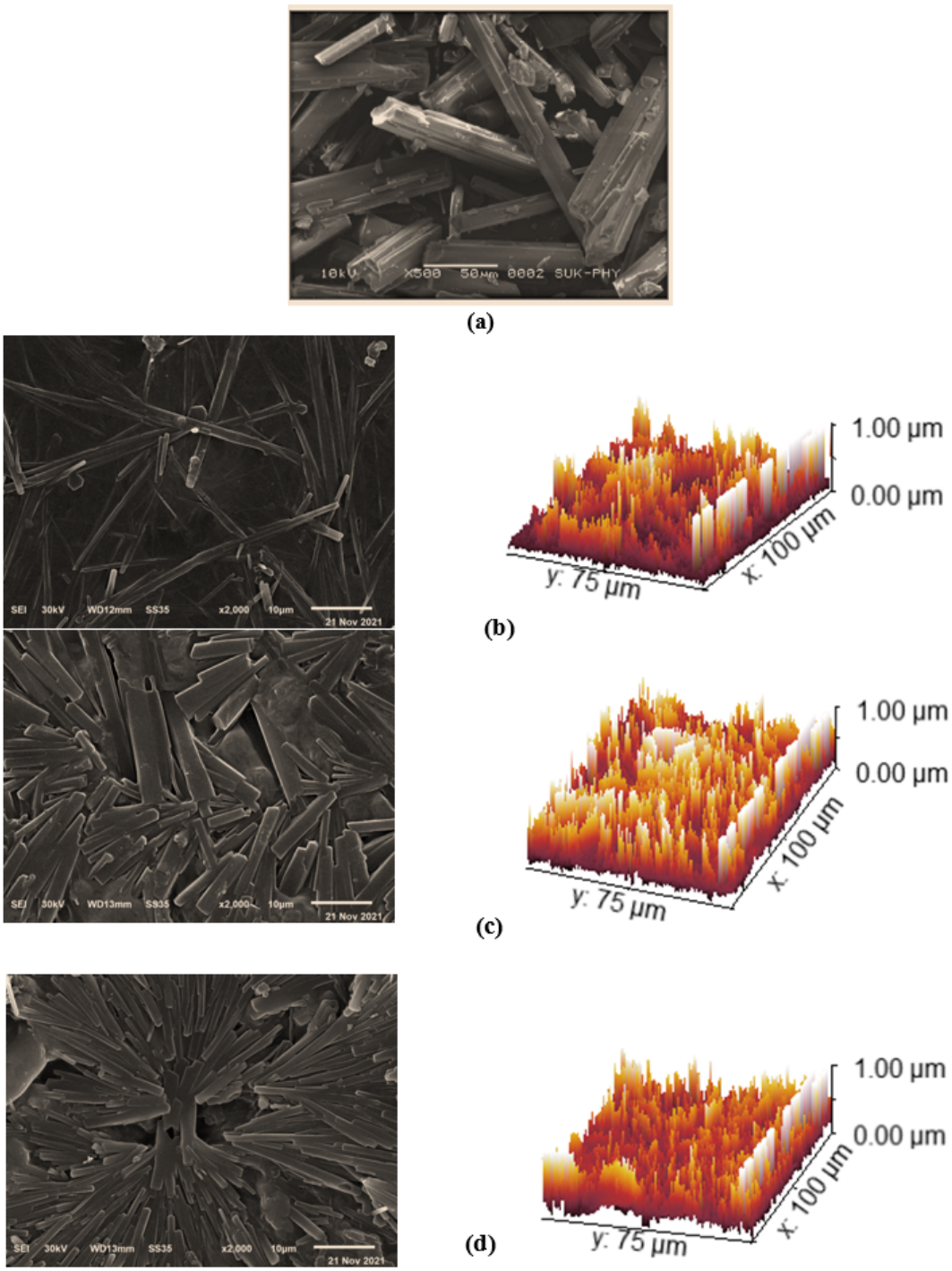

Figure 11

(a-d): Two and three-dimensional images of studied samples: (a) SEM for pure Linezolid drug, (b) SEM for Blend/(0.1ml) Tween(80)/ (20mg/g) Linezolid drug, (c) SEM for Blend/(0.1ml) Tween(80)/ (60mg/g) Linezolid drug and (d) SEM for Blend/(0.1ml) Tween(80)/ (80mg/g) Linezolid drug.

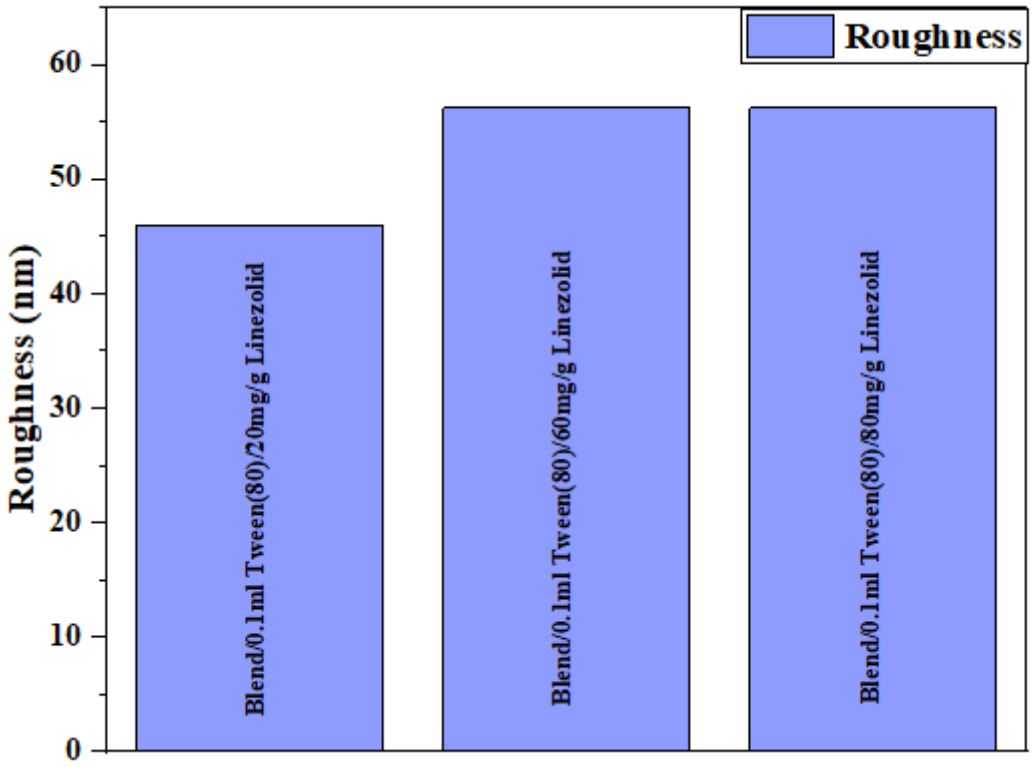

Figure 12

Variation of surface roughness of blend with the addition of different drug content.

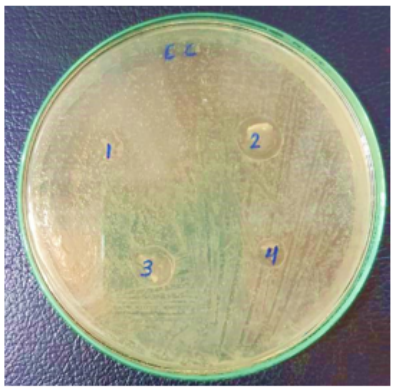

(a)

Effect of *E. coli* on tested samples

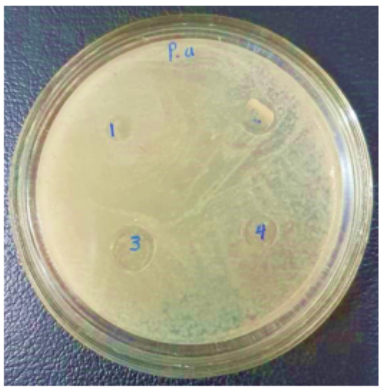

(b)

Effect of *P. aeuroginosa* on tested samples

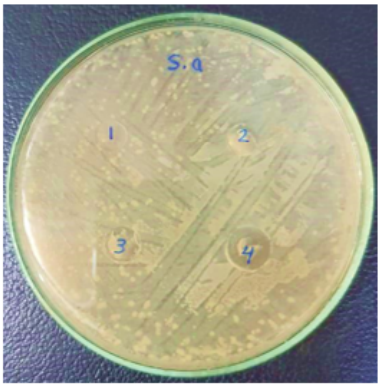

(c)

Effect of *s. au*reus on tested samples

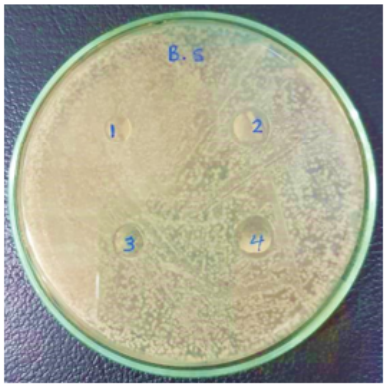

(d)

Effect of *B. subtilis* on tested samples

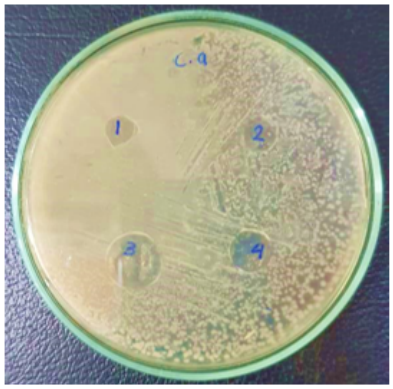

(e)

Effect of *C. albicans* on tested samples

Figure 13

(a-e) Inhibition zones of (blend/(0.1ml) Tween(80)) with different content of drug against various microorganisms

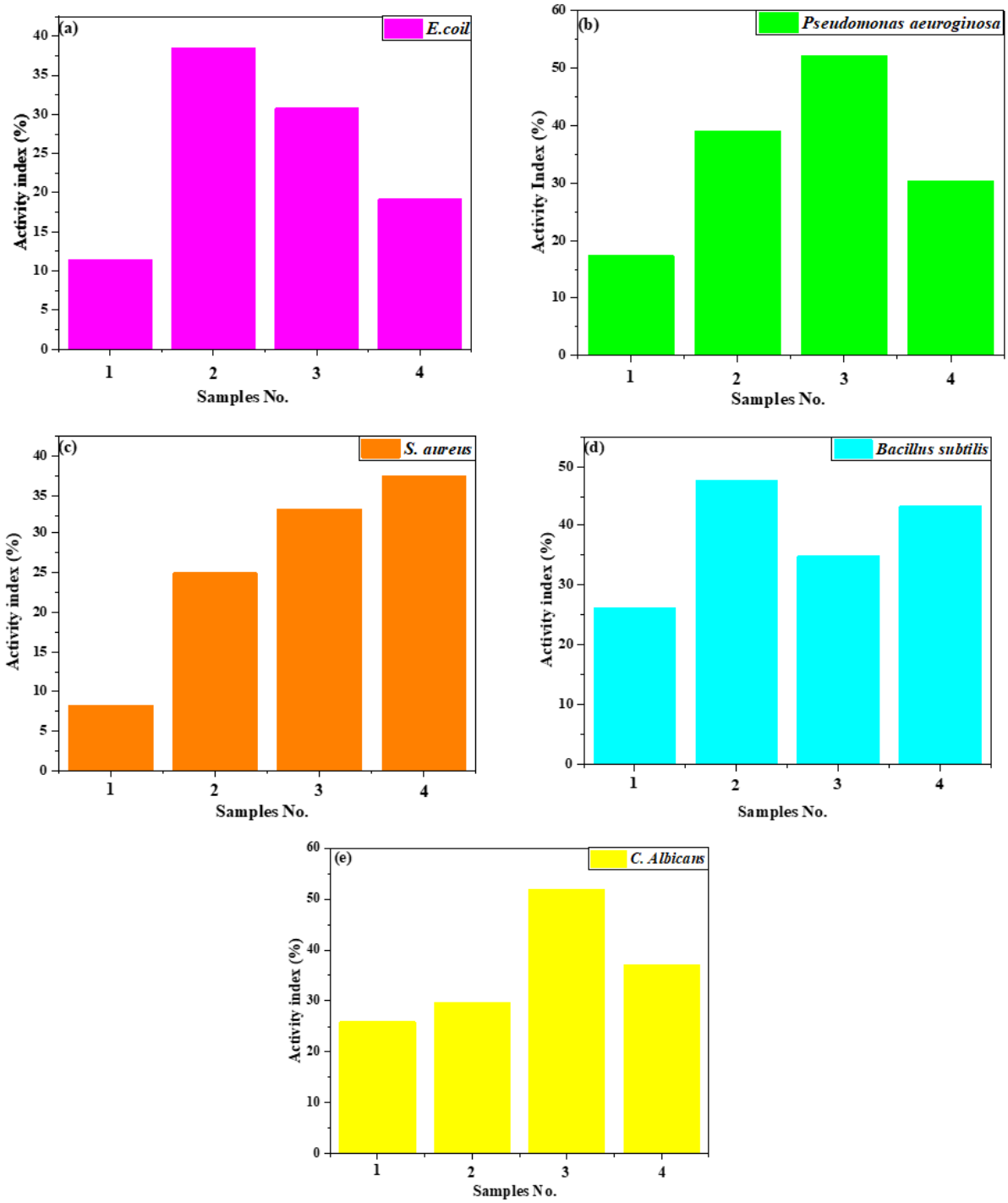

Figure 14

(a-e): Graphic representation of the activity index (%).